3D Reconstruction of *Vitis vinifera* (L.) cvs Pinot Noir and Merlot grape bunch frameworks using a restricted reconstruction grammar based on the stochastic L-system

B. XIN[1], S.LIU[1, 2] and M. WHITTY[1]

[1]School of Mechanical and Manufacturing Engineering, University of New South Wales, 2052 Sydney, Australia; [2]School of Traffic and Transportation Engineering, Central South University, Changsha, Hunan 410075, China

Corresponding author: Dr Mark Whitty, email m.whitty@unsw.edu.au

Short title: 3D reconstruction of grape bunch framework

Abstract

Background and Aims: Phenotypic traits of grape bunches are known to be related with grapevine yield, wine flavour and sensitivity to disease. Aiming to solve a phenotypic bottleneck in current breeding studies as well as improve the performance of phenotypic tools, we put forward a combination of grammar-based reconstruction and vision-based reconstruction, and propose an empirical reconstruction grammar restricted by an outline hull, which can model parameters of the entire bunch framework.

Methods and Results: Statistical analysis of manual measurements of bunches was undertaken to empirically build a reconstruction grammar for a specific grape cultivar. During the reconstruction procedure, the grammar takes account for the estimation of the topological architecture and the geometrical parameters of bunch elements, while the outline hull formed from the input 2D image is used to constrain the volume and the overall shape of the bunch model. The reconstruction results indicated that the average percentage error of quantity estimation for various internode types ranged from 19.1 to 41.1%, and the average percentage error for individual lengths of respective internode types ranged from -0.4 to 10.4%.

Conclusions: The proposed 3D grape bunch reconstruction method achieves the parameter modelling of bunch components by using 2D images as input, and the performance has been shown to be an improvement over existing work.

Significance of the Study: The proposed method enables a more accurate reconstruction of grape bunch framework, from which facilitates the automatic extraction of phenotypic traits and the improvements of breeding programs along with vineyard management. Due to its simple sensor input requirements, it is able to be applied in field conditions.

Keywords: *3D reconstruction, grape bunch framework, reconstruction grammar, stochastic L-system*

Introduction

Phenotypic traits as significant descriptors for plant growth and performance are able to guide research and management in viticulture. Phenotypic traits of berry size and berry number per bunch are considered as two of the important components that contribute to yield estimation (Clingeleffer et al. 2001, Nuske et al. 2011, 2014). Yield estimates are useful for vineyard management (Liu et al. 2015). The size of berries also exerts influences on the flavour of wine, and berries with small to medium size are technically preferred by winegrape breeders for a better red wine quality (Kicherer et al. 2013). The seedlessness of tablegrapes is related to the berry size as well and is proved to be negatively correlated to the berry size, where seedlessness is a significant index in raisin production (Doligez et al. 2002, Fanizza et al. 2005). Apart from this, phenotypic traits of berry volume, internode number, internode length, bunch length and bunch width are closely related with the bunch compactness (Shavrukow et al. 2004, Schöler and Steinhage 2015, Tello et al. 2015, Rist et al. 2018), where the compactness increases the risk of Botrytis infection (Weaver et al. 1962, Vail et al. 1998, Shavrukow et al. 2004) and the susceptibility to the larvae of *Lobesia botrana* (Fermaud 1998). Therefore, effective measures, for instance, gibberellin spraying (Hed et al. 2011) and hand thinning (Barbetti 1980), can be conducted to reduce bunch compactness. In addition, enhanced selection of seedlings and new cultivars is possible as relationships between phenotypic traits and productive indices (flavour, seedlessness and resistance to disease) are known (Herzog et al. 2015).

Although there has been a wide requirement for phenotypic tools, phenotyping at the current stage is beset by measurement methods being labour intensive and time consuming (Herzog 2014), described as the phenotyping bottleneck in Furbank and Tester (2011). 3D bunch reconstruction is a technique that is able to automatically model the inner and outer structure of a bunch which makes the fast extraction of phenotypic traits possible, and provides a feasible solution towards the phenotyping bottleneck. 3D bunch reconstruction techniques focus on presenting a digital model of bunch components, where specific parameters for individual components, for instance, berry size, berry position, internode length and internode orientation, may be taken into consideration according to the input data. Methods of 3D bunch reconstruction have been developed in three classes over the last several decades: grammar-based reconstruction, vision-based reconstruction and scanning-based reconstruction.

As for grammar-based reconstruction, Huang (Huang et al. 2013) established a set of grape bunch generation rules based on an open L-system (Měch and Prusinkiewicz 1996). They added certain geometrical limitations for bunch parameters through a manually defined octahedron, which led to a significant success in both berry reconstruction and internode framework estimation. The main drawback in their method was the assumption that the shape of bunches was always conical while there also exists a large quantity of bunches with funnel shape or cylindrical shape (Organisation Internationale de la Vigne te du Vin 2009). Furthermore, there was no quantitative analysis of their reconstruction result presented, which made it difficult to evaluate its performance compared with other work.

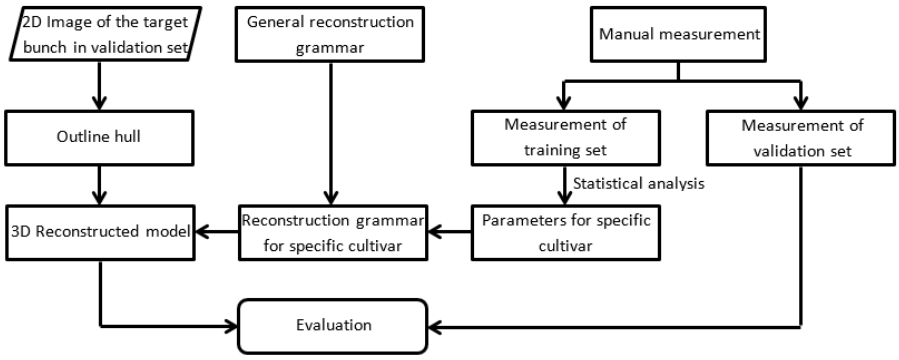

Figure 1. The pipeline of the proposed reconstruction method for modelling of grape bunches. Two main components of the modelling are the outline hull and the reconstruction grammar. Here, the outline hull is extracted from the original 2D image, while the reconstruction grammar is established by integrating general reconstruction rudiments and parameters for specific bunch cultivar obtained from the statistical analysis over manual measurements.

Nomenclature

α	General representation of rotation angle during the first step	E_D	Average error of berry diameter
α_1	Angle between two adjacent internodes on rachis, secondary branches or tertiary branches.	$F1$	An evaluation metric combining precision and recall
α_2	Angle between the first internode on a certain branch and its parent internode	l	General representation of internode length
α_3	Angle between a pedicel and its parent internode	l_0	Initial length of a certain type of internode
β	General representation of rotation angle during the second step	N_E	Average estimated element number with respect to a specified internode type
β_1	Angle between secondary branches at longitudinal level 1 and level 3 (or longitudinal level 2 and level 4)	n_l	Longitudinal level
$\boldsymbol{l_E}$	Length of all internode elements in a reconstruction model with respect to a specified internode type	n_t	Transverse level
$\boldsymbol{l_{GT}}$	Ground truth value of all internode lengths with respect to a specified internode type	N_{FN}	Accumulated false negative value of all reconstruction models with respect to an internode type
a_l	Attenuation rate of internode lengths in longitudinal direction	N_{FP}	Accumulated false positive value of all reconstruction models with respect to an internode type
a_t	Attenuation rate of internode lengths in transverse direction	N_{GT}	Average of actual numbers of a specified internode type
E_o	Overall internode length error with respect to a specified internode type	N_{TP}	Accumulated true positive value of all reconstruction models with respect to an internode type
E_{PI}	Individual internode length error with respect to a specified internode type	P	Precision of a reconstruction model compared with the target bunch
E_{PN}	Percentage error of internode number with respect to a specified internode type	r	General representation of berry radii

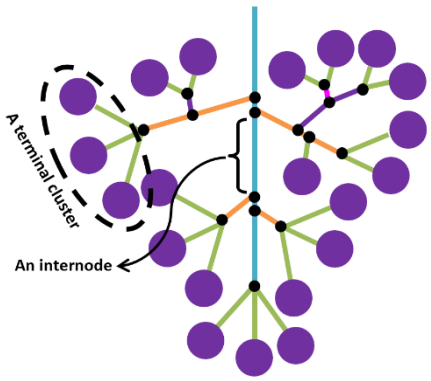

Figure 2. Component decomposition of a grape bunch. Here, internode framework refers to rachis (—), secondary branches (—), tertiary branches (—) and pedicels (—). The overall grape bunch framework includes internode framework and berries ( ). Junctions of internodes are named as nodes (●).

Vision-based methods concentrate on the positional correlation between the reconstructed elements and the corresponding ground truth. A bunch image was captured by a stereo vision system before 3D coordinates of points on berries were obtained through image processing, after which candidate points were arranged into each berry through either sphere fitting or Semi-Global Matching (Herrero-Huerta et al. 2015, Rose et al. 2016). Apart from this, Liu presented a layer-wise berry reconstruction method that arranged berries layer by layer from the end of the peduncle to the bottom of the bunch, where the shape of the boundary of each layer was a circle whose radius was calculated from the outline of the 2D image (Liu et al. 2015). Image-based reconstruction methods are able to provide models whose berry positions match with the ground truth, but they commonly fail to estimate the internode framework inside the bunch because of the occlusion among elements.

Laser scanning as a method which is able to present an accurate point cloud is also employed in 3D bunch reconstruction. From the resulting dense point cloud, Schöler and Steinhage (2015), segmented berries using sphere detection based on the Random Sample Consensus (RANSAC) algorithm (Schnabel et al. 2007). An approximate geometric method was then used to estimate rachis position and secondary branch positions followed by a set of optimisation procedures. Their method achieved a good accuracy in predictions of component number and position. Nevertheless, the prediction of invisible berries was ignored in their work. Apart from this, Rist et al. (2018) achieved the segmentation and the reconstruction of berry elements through a modified algorithm based on the Bunch Analysis Tool (Mack et al. 2017). Modelling, however, of the inner stem system and invisible berries was overlooked. Moreover, 1 min on average was needed to conduct the whole bunch scanning with the laser scanner they used, which limits the application of their method when the number of measurements is large. Furthermore, the requirement of whole bunch scanning is commonly necessary for scanning-based bunch reconstruction methods, while it is usually difficult to rotate the handheld scanner around the target bunch under field conditions because of the dense canopy (Rist et al. 2018).

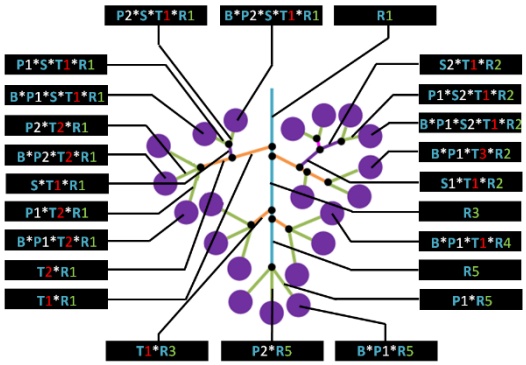

117

118 **Figure 3.** Example of labels for grapevine bunch components as defined in Section Grapevine bunch measurements. Label
119 characters marked by blue refer to internode type abbreviations. Numbers marked by red stand for transverse levels,
120 numbers marked by green stand for longitudinal levels (Section Geometrical reconstruction). A star refers to that the element
121 represented by characters after the star is the parent of the element represented by the whole label.

122

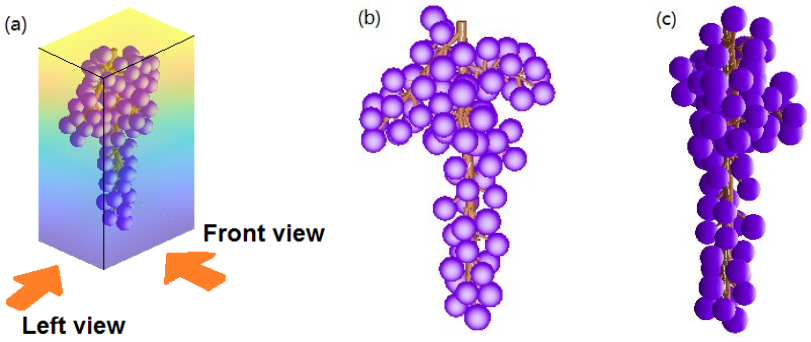

123

124 **Figure 4.** Legend of image capture orientation. Examples of (b) front-view image and (c) left-view image are revealed.

125

126 Since preceding works on bunch reconstruction have limitations in their function, accuracy or
127 experimental condition, we proposed a combination of a grammar-based method and a vision-based
128 method to form an empirical reconstruction grammar. The execution of the reconstruction grammar
129 is restricted by an outline hull generated from a 2D image of the target grape bunch. The final
130 reconstructed model contains four types of information: individual berry position, individual berry size,
131 individual internode length and individual internode orientation. Compared to existing research, the
132 proposed method offers three main benefits:

133 • reconstructed models including both berries and internode framework;

134 • an improved estimation accuracy of element properties; and

135 • requires only a 2D image as sensor input, which is simple to achieve and can be applied under field
136 conditions.

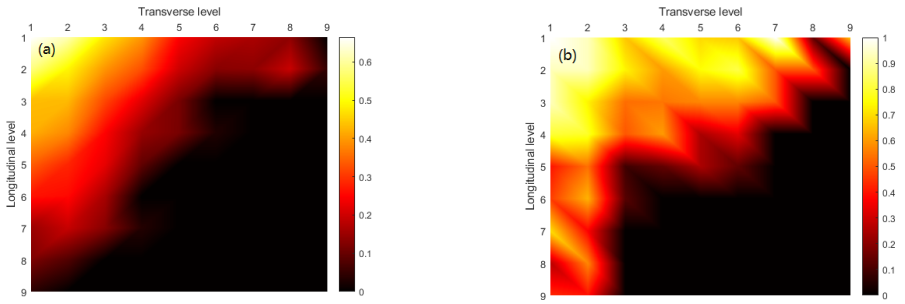

Figure 5. The probability distribution of tertiary branch existence with respect to each node on all potential secondary branches. Colour close to white stands for probability close to 1, while colour close to black represents probability close to 0. Terminology of longitudinal level and transverse level is introduced in Section Geometrical reconstruction. (a) Tertiary branch generation probability of Pinot Noir bunches, (b) tertiary branch generation probability of Merlot bunches.

Materials and methods

The proposed method achieves the modelling of a grape bunch through a reconstruction grammar which stipulates connective relationships among bunch elements as well as parameters of individual bunch element. Here, necessary parameters for specific bunch cultivar were obtained through statistical analysis over the manual measurements. Meanwhile, for the purpose of stipulating the overall volume and the shape of individual bunch models, the execution of the grammar is bounded by a 3D hull generated from the input image, which is also described as the terminal condition. The overall mechanism of the proposed reconstruction method is briefly revealed in Figure 1. Since a uniform terminology of bunch component decomposition does not exist in botanical literature (May et al. 2004, Huang et al. 2013, Schöler and Steinhage 2015), we present a necessary combination of existing terminology in order to make further description (Figure 2).

Grapevine bunch measurements

The original dataset contains 100 *Vitis vinifera* (L.) cv. Pinot Noir bunches and 20 *V. vinifera* (L.) cv. Merlot bunches, where Pinot Noir samples were collected in a vineyard near Blenheim, New Zealand at harvest stage in 2019, while Merlot samples were collected in a vineyard at Cargo, near Orange, New South Wales, Australia at harvest stage in 2018. Among samples within each bunch cultivar, 80% of them were used as the training set which was used to work out general rules of geometrical properties, while the others were used as the validation set whose purpose was to evaluate the performance of the proposed method on specific bunch cultivars.

With respect to a bunch sample, individual berry diameter and internode length was manually measured using a calliper, after which, measurements were recorded in a spreadsheet according to corresponding representations of the elements. Here, the representation is formed by the morphological position (Section Geometrical reconstruction) and the type abbreviation of the element. For a rachis internode, its representation is defined by the letter ‘R’ which stands for the internodes on the rachis, followed by the longitudinal level (Section Geometrical reconstruction). Prefixing that, secondary internodes are represented by the letter ‘T’ which stands for the internodes on the

secondary branch, together with the transverse level (Section Geometrical reconstruction). This is further prefixed by the letter 'S' which stands for the internodes on the tertiary branch, which is optional depending on whether it exists. Pedicels are then represented by the letter 'P', followed by the index of the pedicel where more than one exists at the same node. Prefixing this is the letter 'B' to represent a berry on a pedicel. Thus, label 'B*P1*S*T1*R1' in Figure 3 represents the berry on the first pedicel on a single tertiary branch on the first internode of the secondary branch after the first rachis internode. Further examples of labelling for bunch components are shown in Figure 3.

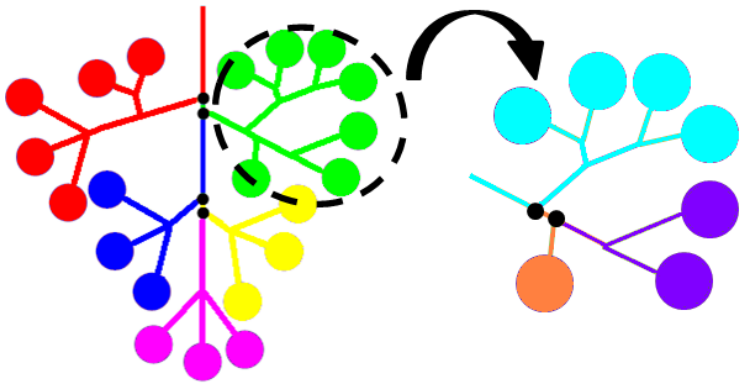

Figure 6. Division of bunch elements with respect to longitudinal and transverse direction. Longitude level one (—), longitude level two (—), longitude level three (—), longitude level four (—), longitude level five (—). For revealing the division with respect to transverse direction, we only take the secondary branch marked with a dashed circle as an example, and it is similar to other secondary branches. Transverse level one (—), transverse level two (—), and transverse level three (—).

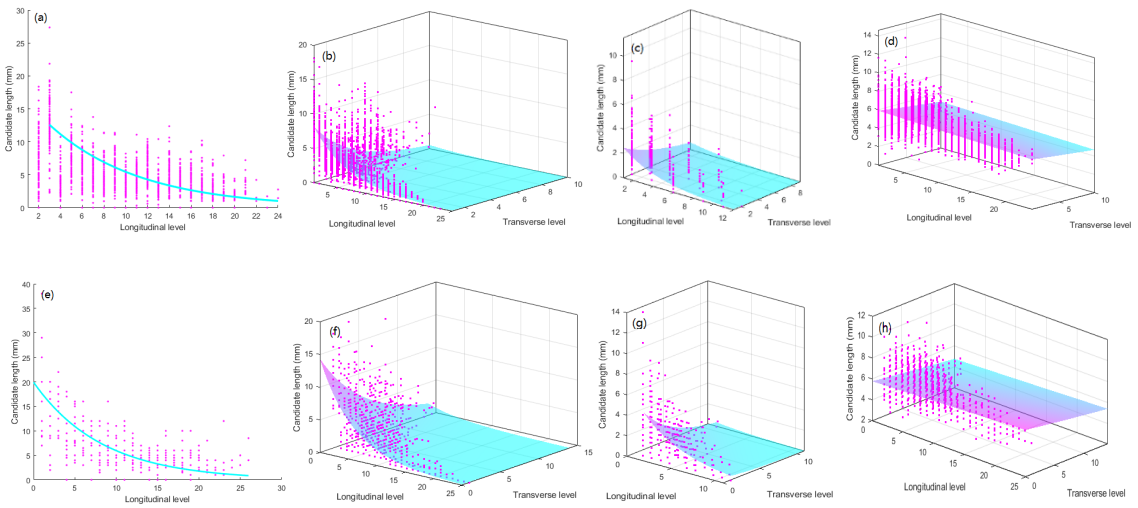

igure 7. Internode length attenuation for (a,e) rachis, (b,f) secondary branch), (c,g) tertiary branch and (d,h) pedicel. (a,b,c,d) Images reveal internode length attenuation of Pinot Noir bunches, (e,f,g,h) images reveals internode length attenuation of Merlot bunches.

A 2D front-view image was captured for each individual bunch sample in outdoor environment under an umbrella (to minimise harsh shadows) with an RGB camera on a smartphone giving images of a resolution of 3120×4160 pixels. Noticed that different image capture orientations will give rise to different bunch outlines (Figure 4), left view images were also captured for Merlot bunches in order to figure out the influence of image capture orientations on the overall reconstruction result. A chequerboard was placed behind the target bunch to facilitate the image noise removal and camera calibration (Figure 9a). Examples of raw images captured with front view and left view are shown in Figure 11.

The algorithm was developed and tested with MATLAB (version: R2017a) on a desktop computer with a 3.2GHz processor and 16GB RAM.

Reconstruction grammar

The proposed reconstruction grammar is a combination of topological rudiments and geometrical rudiments that describes the general rule of bunch architecture. Here, topological rudiments refer to the connective relationship among internodes (Godin 2000), while geometrical rudiments stand for the parameter quantisation of individual elements.

Topological reconstruction. Knowing the decomposition information (Godin 2000) of bunch components, topological reconstruction aims to define the connection among different components. The reconstruction starts from the hypoclade which connects to the shoot (Pratt 1971), and continues through all rachis internodes down to the base of the grape bunch approximately along its axis of symmetry. Branches generated at nodes on the rachis are secondary branches (Troll 1964) from which tertiary branches or pedicels arise. The selection of tertiary branch or pedicel at a node on a secondary branch is determined by the probability obtained from statistical analysis of measurements. With respect to each longitudinal level and transverse level, the proportion of bunch samples which hold a tertiary branch was calculated by searching with internode representations within measurement forms (Section Grapevine bunch measurements). The generation probability distributions of a tertiary branch at each morphological position for respective bunch varieties are then presented in Figure 5, where a significant decrease of the tertiary branch existence probability is observed along the rachis. Importantly, bunches with different shapes and cultivars indicate different probability distributions of tertiary branch existence. Terminal clusters then arise at the termination of rachis and each branch while a single berry is created at the end of each pedicel. According to the data analysis over measurements, the number of pedicels within a terminal cluster obeys a uniform distribution of $\mathrm{U}(1, 8)$. In normal condition, pedicels and berries are one-to-one matched with each other unless berries had fallen off.

Geometrical reconstruction. Having the topological model of a bunch, the purpose of geometrical reconstruction is to stipulate geometrical parameters for each bunch element. Here, geometrical parameters refer to lengths and orientations for internode elements or berry diameters for berry elements.

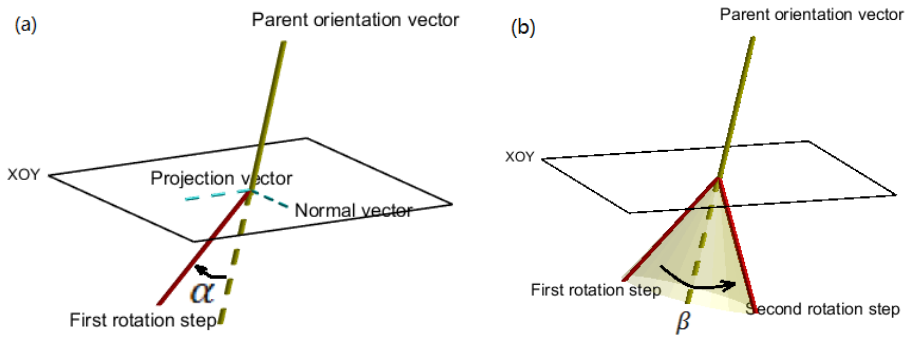

225

226 **Figure 8.** Description of the two steps of rotation operations applied in this paper. (a) The first rotation step: parent
227 orientation vector rotates around its normal vector on plane XOY. (b) The second rotation step: result of the first step rotates
228 around the parent orientation vector.

229 **Table 1.** Attenuation rates of internode length for respective internode types derived from manual
230 measurement of grapevine bunches.

Internode type	Attenuation direction	a_l		a_t		l_0 (mm)	
		Pinot Noir	Merlot	Pinot Noir	Merlot	Pinot Noir	Merlot
Rachis	Longitudinal	0.89	0.88	1.00	1.00	12.58	15.29
Secondary branch	Both	0.84	0.83	0.74	0.86	8.20	10.54
Tertiary branch	Both	0.75	0.80	0.84	0.79	2.45	4.26
Pedicel	Transverse	1.00	1.00	0.98	0.97	5.88	5.70

231 a_l, the attenuation rate in longitudinal direction; a_t, the attenuation rate in transverse direction; l_0, the initial length of
232 the respective internode type.

233

234 To illustrate this further, an introduction of morphological division of bunch elements is necessary.
235 In longitudinal direction, bunch elements are divided into different levels by setting breakpoints at
236 nodes on the rachis, where each level consists of a rachis internode as well as all its child elements
237 (internodes of secondary branches, tertiary branches, pedicels and berries), as is shown in Figure 6.
238 The level close to the apex of the bunch is considered as the first longitudinal level (marked in red in
239 Figure 6) and all levels progressively increase down to the lowest node of the rachis. Similarly, in the
240 transverse direction, elements are also classified into different levels by taking nodes on secondary
241 branches as breakpoints. Therefore, each transverse level contains corresponding internodes on each
242 secondary branch as well as their child elements (internodes of tertiary branches, pedicels and berries),
243 as is shown in Figure 6. Here, we specify the first transverse level as the one that is connected with
244 the rachis (marked in light blue in Figure 6), and all levels increase progressively until the last node on
245 a secondary branch.

246 **Internode length.** By extracting corresponding length measurements with respect to internode types
247 and bunch cultivars, the curve fitting method was used to model internode length and an obvious
248 attenuation phenomenon was found with ascending morphological levels. It is worthwhile to mention
249 that the length attenuation of rachis internodes only relates to the ascending of the longitudinal level
250 (Figure 7a,e), while attenuation rate of pedicel internode lengths indicates a closer correlation with

the transverse level than the longitudinal level (Figure 7d,h). Lengths of the other two types of internodes (secondary branches and tertiary branches) reveal attenuation in both the longitudinal direction and the transverse direction, as is shown in Figure 7b, c, f, g. By adding uncertainties on the attenuation term to simulate the randomness in nature, the length of each internode is represented by Equation 1:

$$l = l_0 \times a_l^{n_l - 1} \times a_t^{n_t - 1} + \xi, \quad (1)$$

where l_0 is the initial length (Table 1) obtained by taking the average length of all internodes of a specified internode type over the training set whose longitudinal level and transverse level are both equal to one; a_l and a_t represent the attenuation rate in longitudinal direction and transverse direction respectively (Table 1); n_l and n_t stand for longitudinal level and transverse level respectively; and ξ represents uncertainties. Here, the uncertainties are assumed to obey a normal distribution whose Standard Deviation (SD) is calculated from the training set.

Internode orientation. Orientation is the other property necessary during the creation of an internode element. Here, we propose a better way to determine the internode orientation than the one previously used (Prusinkiewicz 2001, Huang 2013). The orientation of an internode is derived from its parent orientation vector by applying two steps of rotation. During the first step, a rotation of the parent internode orientation vector around its normal vector is conducted, where the normal vector is the perpendicular vector of the parent orientation vector on plane XOY (Figure 8a). Subsequently, the result of the first step is rotated around the parent internode orientation vector to form a new orientation vector for the child internode (Figure 8b). The rotation angle in the first step is interpreted as the angle between two internodes while the rotation angle in the second step is interpreted as the direction of branch growing trend, as is revealed in Figure 8. Compared with rotation operation in traditional L-system whose rotation operations were around x, y and z axes (Prusinkiewicz et al. 2001), the proposed rotation rule not only simplifies the logic, but is able to make the creation of internodes more understandable as well. Following the above rotation principles, the probable position that a child internode is created should be an area with cone shape by given the parent internode orientation as well as the angle between the child internode and its parent, as is shown in Figure 8b. For the purpose of increasing the diversity of bunch models being reconstructed, necessary rotation angles in this paper are assumed to obey normal distributions whose expectations and SDs are presented in Table 2. These were obtained by inspection of bunches during decomposition.

Berry diameter. Instead of a significant attenuation with the increase of morphological level, the diameter of berries indicates a slight fluctuation around the expected value according to statistical analysis over manual measurements. In this paper, berry diameter of Pinot Noir bunches was set to obey a Gaussian distribution of $\mathcal{N}(10.36, 1.17)$, while a distribution of $\mathcal{N}(11.25, 0.93)$ was obtained using Merlot bunches.

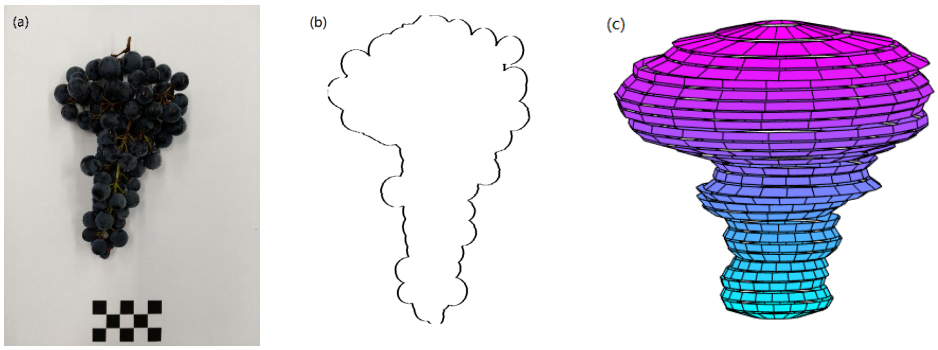

Figure 9: Generation steps of outline hull. (a) The image of target the grapevine bunch. (b) The boundary image of the target bunch. (c) The outline hull of the target grapevine bunch formed by integrating truncated cones of each slice.

Table 2. Rotation angles for internode creation.

Type of angle	μ (Degrees)	σ (Degrees)
α_1	0	5
α_2	75	5
α_3	45	5
β_1	90	10

μ, expected value; σ, SD; α_1, the angle between two adjacent internodes on rachis or secondary branches or tertiary branches; α_2, the angle between the first internode on a certain branch and its parent internode; α_3, the angle between a pedicel and its parent internode; β_1, the angle between secondary branches at longitudinal level 1 and level 3 (or longitudinal level 2 and level 4) as defined and observed by May et al. (2004).

Table 3. Interpretation of symbols used in turtle graph.

Symbol	Interpretation
∨	Rotation around the normal of parent orientation vector counter-clockwise
∧	Rotation around the parent orientation vector counter-clockwise
$C(l)$	Draw a cylinder at current position along current orientation with length l
$S(r)$	Draw a sphere at current position with radius r
[	Push current state into the stack
]	Pop a state from the stack

Algorithm 1. Restricted reconstruction grammar.

function $RACHIS$
  while 1 **do**
    for $nAttempt = 0$ to 100 **do**
      $\vee\ (\alpha) \wedge (\beta) C(l)$
      if Do NOT exceed the boundary **then**
      $[SECONDARY]$
      break
      end if

```
        end for
        if Still exceeding the boundary then
          break
        end if
      end while
    [TERMINAL_CLUSTER]
end function

function SECONDARY
      while 1 do
        for nAttempt = 0 to 100 do
          ∨ (α) ∧ (β)C(l)
          if Do NOT exceed the boundary then
            [TERTIARY or PEDICEL]
            break
          end if
        end for
        if Still exceeding the boundary then
          break
        end if
      end while
      [TERMINAL_CLUSTER]
end function

function TERTIARY
   for nAttempt = 0 to 100 do
     ∨ (α) ∧ (β)C(l)
       if Do NOT exceed the boundary then
         [TERMINAL_CLUSTER]
         break
     end if
   end for
end function

function PEDICEL
   for nAttempt = 0 to 100 do
     ∨ (α) ∧ (β)C(l)[S(r)]
     if Do NOT exceed the boundary then
       [S(r)]
       break
     end if
   end for
end function

function TERMINAL_CLUSTER
   for n_p = 0 to nPedicels do
     [PEDICEL]
   end for
end function
```

α, β, l and r are the general representations of rotation angle of first step, rotation angle of second step, internode length and berry radius respectively, which need to be specified by applying Equation 1, Table 1 or Table 2.

Terminal condition

Given the reconstruction grammar which contains topological and geometrical rudiments of bunch architecture, the generation of bunch elements is limited by an outline hull extracted from a 2D image of the target bunch. The function of the outline hull is to constrain the volume and the overall shape of the bunch model, and consequently, it is also taken as the terminal condition during the execution of the reconstruction grammar.

The method proposed by Font (2015) is used to generate an outline hull of a target bunch. The boundary image of a grape bunch (Figure 9b) is divided into 50 equal slices along its central axis of symmetry before a truncated cone for each slice is formed using its maximum radius and minimum radius. A smooth outline hull of the target bunch outline is able to be generated by integrating all these truncated cones together (Figure 9c).

Here, an algorithm is presented to describe the reconstruction mechanism of grape bunches (Algorithm 1). In the proposed algorithm, an L-system is employed combining with pseudo-code and turtle graph which simplifies motions of each step as a string (Prusinkiewicz et al. 1994, Měch et al. 1996). Table 3 presents an interpretation of symbols.

Evaluation metrics

For the purpose of assessing the performance of the proposed reconstruction method, we present a set of evaluation metrics from aspects of element quantity, bunch topology and candidate length. Considering the randomness in reconstruction grammar, 100 attempts of reconstruction were conducted based on a reference image of each bunch in the validation set. Corresponding evaluation metrics were then calculated for each bunch from these 100 reconstructed models.

Element quantity. The evaluation of element quantity aims to compare the estimated number of elements of respective internode types with the corresponding actual numbers. In order to have a parallel comparison with other articles, the percentage error of the number of element with respect to each internode type is presented by Equation 2:

$$E_{PN} = \left|\frac{N_E - N_{GT}}{N_{GT}}\right| \times 100\% \quad (2)$$

where N_E represents the average estimated number of element with respect to a specified internode type, and N_{GT} stands for the average of corresponding actual numbers.

Bunch topology. The evaluation of bunch topology verifies the performance of the proposed method from the aspect of the existence of individual elements that appear in the target (actual) bunch. Hereby, individual elements in both reconstructed models and target bunches are given a unique representation which consists of its morphological position information as well as internode type abbreviation (Sections Grapevine bunch measurements and Geometrical reconstruction). Then, an element association between a reconstruction model and the target bunch is conducted according to

their representations. Both matched and non-matched candidates are marked in this procedure and the topology accuracy is then described by precision, recall and $F1$ score. Before the introduction of topology evaluation metrics, definitions of true positive, false positive and false negative are mentioned in the context of our experimental environment. The true positive value refers to the number of estimated elements that matches with the actual elements in the target bunch. The false positive value stands for the number of elements in the reconstructed model that do not match with the actual elements in the target bunch. The false negative value represents the number of actual elements in the target bunch that do not match with the estimated elements.

- *Precision*. This is a metric measuring the proportion of elements that are estimated correctly, which is derived from Equation 3:

$$P = \frac{N_{TP}}{N_{TP}+N_{FP}}, \tag{3}$$

where N_{TP} and N_{FP} are the accumulated true positive value and false positive value respectively within all reconstruction models with respect to a specified internode type.

- *Recall*. The recall metric stands for the proportion of actual candidates that are successfully estimated. It is derived from the proportion of correct estimation number and actual candidate number, as is described in Equation 4:

$$R_e = \frac{N_{TP}}{N_{TP}+N_{FN}}, \tag{4}$$

in which N_{FN} stands for the accumulated false negative within all reconstruction models with respect to a specified internode type.

- $F1$ *Score*. This is an evaluation metric indicating the overall performance of topology reconstruction by combining precision and recall (Equation 5):

$$F_1 = \frac{2 \cdot P \cdot R_e}{P+R_e}, \tag{5}$$

The overall performance will be better if $F1$ score is closer to 1, and vice versa.

Element properties. Evaluation of element properties was conducted within three aspects - overall internode length error, individual internode length error and average error of berry diameter. They were calculated as follows.

- *Overall internode length error* (E_O). This evaluation criteria was first presented by Schöler (2015), which represented the difference of overall internode length with respect to a specified internode type between a reconstructed model and the ground truth (Equation 6):

$$E_O = \sum \boldsymbol{l_E} - \sum \boldsymbol{l_{GT}}, \tag{6}$$

where $\boldsymbol{l_E}$ is a vector storing the lengths of all internodes in a reconstructed model with respect to a specified internode type, and $\boldsymbol{l_{GT}}$ stores the corresponding ground truth values.

- *Individual internode length error* (E_{PI}). For a specified internode type, E_{PI} refers to the weighted percentage error of individual internode length compared with corresponding ground truth values. It can be derived from Equation 7 after an element association procedure is applied:

$$E_{PI} = \sum \frac{\boldsymbol{w_i}(\boldsymbol{l_{E_i}} - \boldsymbol{l_{GT_i}})}{\boldsymbol{l_{GT_i}}} \times 100\%, \quad (7)$$

in which i represents the element index in each reconstructed model with respect to a specified internode type. Here, a weight vector $\boldsymbol{w}$ which contains weight factor for each internode is added to balance the impact of internode length difference exerted on final percentage length error (Equation 8):

$$\boldsymbol{w} = \frac{\boldsymbol{l_{GT}}}{\sum \boldsymbol{l_{GT}}}. \quad (8)$$

- *Average error of berry diameter* (E_D). From 100 attempts of reconstruction with respect to a target bunch, the average error of berry diameter is defined as Equation 9, where D_i refers to the determined berry diameter, D_{GT} refers to the corresponding berry diameter in the real bunch:

$$E_D = \frac{\sum |D_i - D_{GT}|}{100} \quad (9)$$

Results and discussion

According to the proportion mentioned in Section Grapevine bunch measurements, 20 bunches of Pinot Noir and four bunches of Merlot were selected as the validation set. The reconstruction results of the proposed method were partially illustrated in Figures 10, 11a,c, respectively, by using 2D front-views images as inputs. For the sake of visualising the function of outline hulls, they are also displayed in Figure 10. The average time duration for a single bunch reconstruction was 36.9s employing the aforementioned hardware and algorithm.

The overall performance of the proposed method over Pinot Noir samples and Merlot samples is summarised in Table 4 by taking the average value of each evaluation metrics proposed in Section Evaluation metrics, and corresponding specific results for respective bunch varieties are described in the following subsections. Whereas Schöler (2015) present the only measure of accuracy for detailed grape bunch reconstruction, we present a detailed comparison with their results. Apart from this, the influence of different image capture orientations on the final reconstruction performance is also presented and discussed.

Element quantity

From 100 reconstruction attempts for each target bunch using the front-view image, the percentage errors of estimated number of internodes for respective candidate types were calculated according to Equation 2, and then averaged with respect to bunch cultivars. Corresponding performance is revealed in Table 5. Here, berry counts are not mentioned separately because the number of berries is equal to that of pedicel internodes according to the aforementioned reconstruction grammar (Algorithm 1).

405

406

407

408

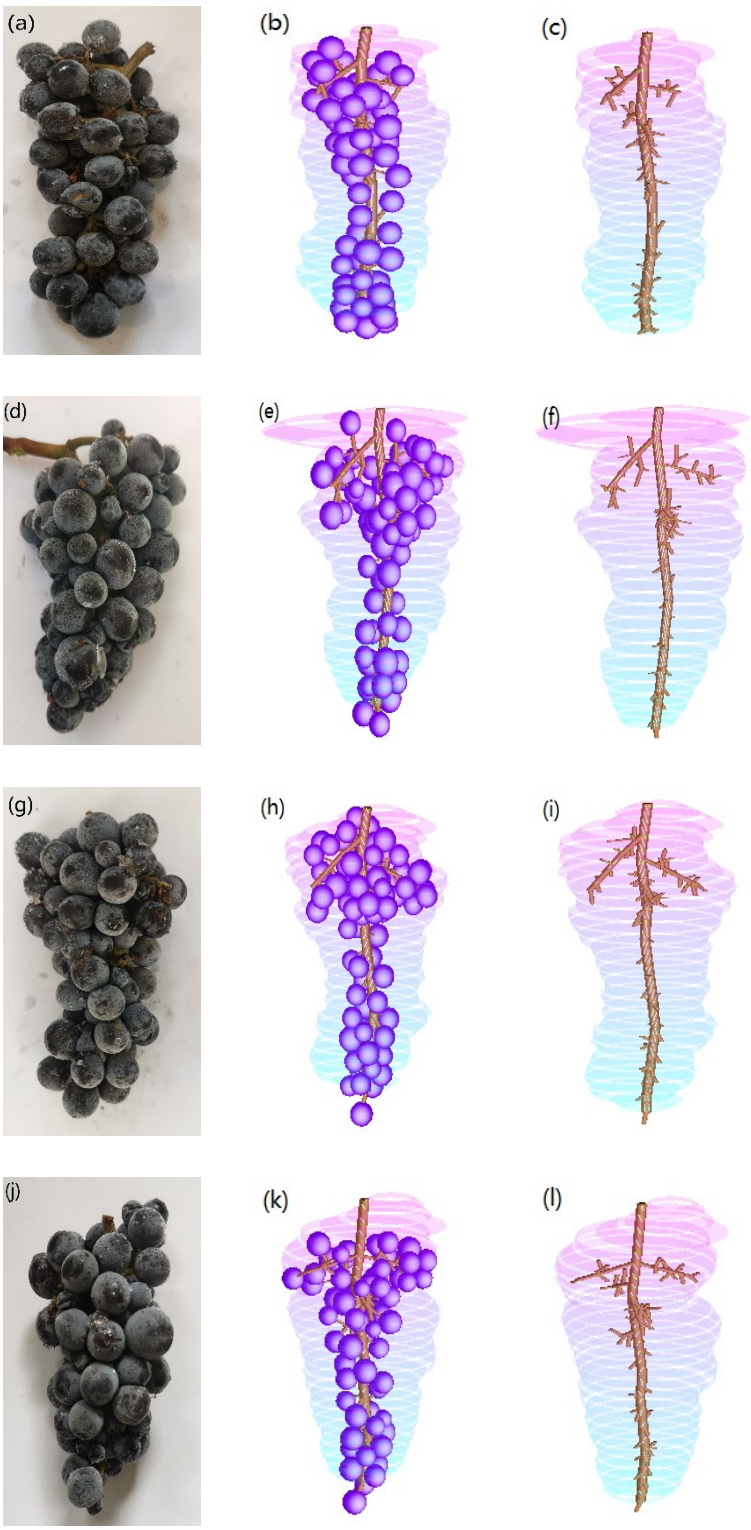

409 **Figure 10.** Reconstruction results of the proposed method over Pinot Noir bunches using front-view images, showing (a,d,g,j)
410 raw images of target bunches, (b,e,h,k) overall bunch reconstruction results and (c,f,i,l)_internode framework reconstruction
411 results.

412

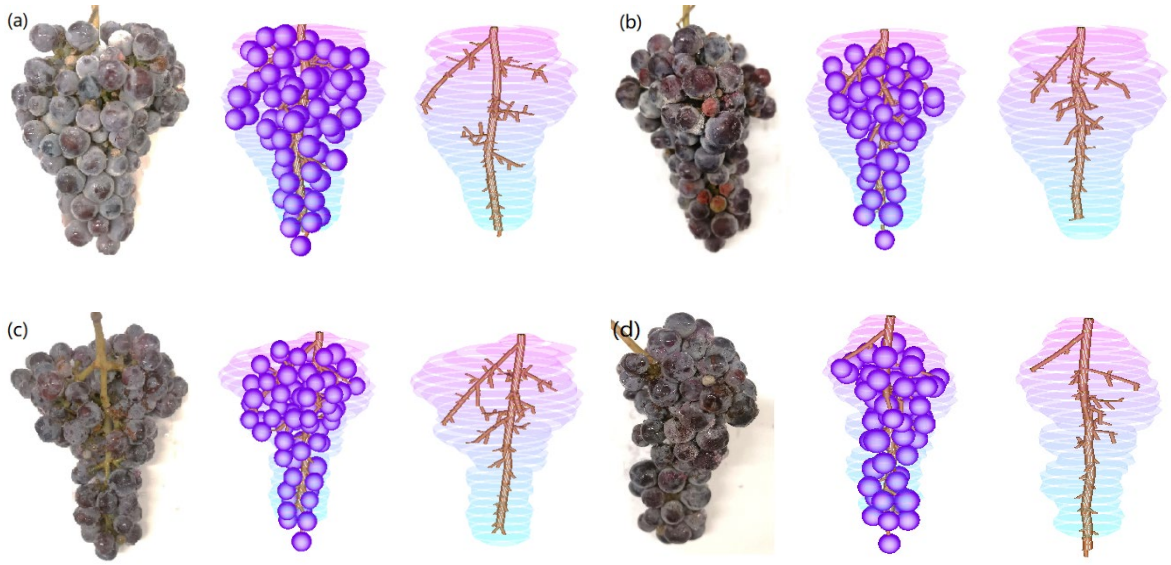

Figure 11. Reconstruction results of the proposed method over Merlot bunches using images captured from (a,c) front-view images, (b,d) and from corresponding left-view images.

Table 4. Summary of the overall reconstruction performance using front-view images with respect to internode types (bunch cultivar: Pinot Noir and Merlot)

Evaluation metrics	Rachis	Secondary	Tertiary	Pedicel
Percentage error of internode number per bunch (%)	22.1	19.1	34.0	41.1
$F1$ Score	0.87	0.75	0.44	0.37
Percentage error of overall internode length (%)	4.3	6.7	-28.5	-42.9
Percentage error of individual internode length (%)	-0.4	10.4	-9.1	-9.4

Combining the reconstruction performance over two bunch cultivars, the average absolute errors with respect to rachis internodes, secondary branch internodes, tertiary branch internodes and pedicel internodes were 4.1, 7.1, 5.3 and 40.4, respectively. The average percentage errors of internode number for respective internode types were 22.1, 19.1, 34.0 and 41.1%, respectively. Compared with results presented by Schöler (2015), which were 25.0, 20.4, 50.5 and 12.8%, respectively, our reconstruction result illustrates a greater accuracy in estimations of rachis internodes, secondary branches and tertiary branches, while a lower accuracy is shown in estimations of pedicel internodes. The lower estimation accuracy of pedicel internode number is mainly caused by the space utilisation around the boundary of the outline hull. As is shown in Figure 9b, there are many berries which support the outline positioning at the edge of the bunch. It is difficult for a grammar-based reconstruction method to fit berries near the complex boundary because it is easier to cause a collision with the outline hull, which lays a foundation for the future improvement. Apart from this, reconstruction of tertiary branches also indicates a large percentage error. This is mainly caused by the probability distribution of tertiary branch existence that we employed is not accurate enough. In order to improve this, a more suitable probability models rather than Gaussian distribution will be considered in the future version.

436

437 **Table 5.** The percentage error of estimated number of internodes per grapevine bunch for
438 respective internode types.

Internode type	Ground truth average†	Average error‡	Percentage error (%)§
Merlot			
Rachis	19.5	5.5	28.3
Secondary	64	8.0	13.3
Tertiary	25.8	8.1	35.7
Pedicel	133.5	35.5	26.4
Pinot Noir			
Rachis	18.3	3.8	20.8
Secondary	35.7	6.9	20.2
Tertiary	11.7	4.7	33.7
Pedicel	93.4	41.4	44.0

439 With respect to individual internode type, † average actual number, ‡the average error of estimated internode number, §
440 the corresponding average percentage error.

441

442 By comparing the reconstruction result between Pinot Noir bunches and Merlot bunches, Merlot
443 samples usually indicates a better reconstruction performance in aspect of candidate quantity using
444 the proposed reconstruction method. This is due to the difference between bunch compactness.
445 According to Organisation Internationale de la Vigne et du Vin (2009), Merlot bunches normally reveal
446 a compactness factor of 3 to 5 while a compactness factor no less than 7 is usually obtained with Pinot
447 Noir bunches. A tighter bunch means a higher inner space utilisation rate. However, grammar-based
448 reconstruction methods employ a strategy of randomly positioning candidates within a feasible space
449 instead of a well-organised space utilisation, which will waste a large amount of space. Therefore,
450 future improvements will be employed to increase the inner space utilisation rate in order to improve
451 the reconstruction performance on tight bunches.

452 *Bunch topology*

453 The evaluation on bunch topological reconstruction concentrates on the element coincidence
454 between a reconstructed model and the corresponding real bunch. In this paper, precision, recall and
455 $F1$ score, as descriptors indicating the existence of internode candidates that are supposed to appear
456 in reconstruction models, were introduced and applied to assess the proposed reconstruction method.
457 From 100 reconstructed models of each target bunch using the front-view image, the precision, recall
458 and $F1$ score were calculated over respective bunch cultivars using method proposed in Section
459 Element quantity, and the results are illustrated in Table 6.

460

461

462

Table 6. Performance of bunch topology estimation evaluated by metrics of precision, recall and $F1$ score.

Internode type	Precision (%)	Recall (%)	$F1$ Score
Merlot			
Rachis	76.5	99.5	0.87
Secondary	82.4	81.3	0.82
Tertiary	68.4	62.7	0.64
Pedicel	55.9	41.7	0.48
Pinot Noir			
Rachis	82.8	93.7	0.87
Secondary	75.0	72.4	0.73
Tertiary	49.3	33.0	0.40
Pedicel	47.3	26.7	0.35

Combining the performance over two bunch cultivars, the average precision of estimation of rachis internodes, secondary internodes, tertiary internodes and pedicel internodes was 81.8, 76.2, 52.5 and 48.7%, respectively. The average recall of respective internode types were 94.7, 73.9, 38.0 and 29.2%, respectively. The average $F1$ scores were 0.87, 0.75, 0.44 and 0.37 for respective internode types. According to the above values of assessment criteria, the proposed method indicates a high confidence in rachis candidate estimation and secondary candidate estimation, while less accurate results were obtained on tertiary candidate estimation and pedicel candidate estimation. We notice the phenomenon that the reconstruction performance revealed a gradually decreasing trend as the branching level going from rachis to pedicel. The main factor contributing to this was the uncertainty during generation of candidates at each node. As is mentioned in Section Topological reconstruction, the probability distribution of branch generation is assumed to be independent, which means that the uncertainty should ascend as the branching level becomes higher because of the uncertainty accumulation. The increase of uncertainty directly gave rise to the increase in error.

Due to the complexity and randomness in grape bunch architecture, criteria of bunch topology present a higher challenge for grape bunch reconstruction methods. To the best of the authors' knowledge, this is the first time that the element-wise topology comparisons are applied to the evaluation of 3D grapevine bunch reconstruction. Since there has not been any other work published in this field, no parallel comparison can be presented.

Element properties

Within 100 reconstructed models of each target bunch using the front-view image, the average error of overall internode length with respect to each internode type was obtained by applying Equation 6 to each reconstruction model and then taking the average of these. The error of individual internode lengths with respect to the internode type was obtained by averaging the results of Equation 7 applied to each reconstruction model. And the average error of berry diameter was calculated by employing Equation 9. For the purpose of parallel comparison, the percentage error of overall internode length was also calculated by using overall length error divided by corresponding groundtruth value. Average

errors of individual internode length and overall internode length for respective bunch cultivars are illustrated in Table 7 and Table 8, respectively.

Table 7. Internode individual length with respect to internode types of grapevine bunches.

Internode type	Percentage error (%)
Merlot	
Rachis	-2.8
Secondary	2.4
Tertiary	-24.3
Pedicel	3.8
Pinot Noir	
Rachis	0.1
Secondary	-12.9
Tertiary	-6.1
Pedicel	-12.0

Table 8. Internode overall length with respect to internode types of grapevine bunches.

Internode type	Ground truth average (cm)†	Average error (cm)‡	Percentage error (%)§
Merlot			
Rachis	13.5	-0.2	-1.3
Secondary	23.4	5.4	23.4
Tertiary	5.6	-0.5	-5.7
Pedicel	77.5	-2.2	-2.9
Pinot Noir			
Rachis	9.7	0.4	5.4
Secondary	11.9	-1.9	-12.7
Tertiary	2.1	-0.9	-33.1
Pedicel	54.5	-27.9	-50.9

†Average actual values of the overall internode lengths of respective internode types; ‡average errors of overall internode lengths; § the average percentage errors of overall internode lengths.

In terms of individual internode length, the average percentage errors of respective internode types were -0.4, 10.4, -9.1 and -9.4%, respectively, which indicated that the estimation of individual internode length was accurate enough. This was mainly due to the prior knowledge provided by statistical analysis over internode actual length in training set, which also suggested that our hypothesis of probability distribution of candidate length was confirmed under real conditions. As this is the first time that an element-wise evaluation of internode length in area of 3D bunch reconstructions has been introduced, no parallel comparison can be presented.

From the aspect of overall length error, the average error of rachis internodes, secondary internodes, tertiary internodes and pedicel internodes was respectively, 0.3, -0.7, -0.8 and -23.6 cm. Then, the corresponding percentage errors were 4.3, 6.7, -28.5 and -42.9%, respectively. The estimation of rachis and secondary internode overall length is accurate enough, and compared with the reconstruction method presented in Schöler (2015) whose overall percentage

length error of secondary branch internodes was 29.6%, the proposed method was substantially better. Since the compactness of a bunch can be derived from the overall length of rachis internodes and secondary internodes (Shavrukow et al. 2004, Schöler and Steinhage 2015), and the compactness of a bunch is closely related with the sensitivity of pests and diseases, a higher accuracy of overall internode length estimation will consequently contribute to the study on disease control and guide further phenotype improvements through breeding efforts. Nevertheless, the performance of overall length estimation of tertiary internodes and pedicels with respect to Pinot Noir samples demonstrate a slight lower accuracy. Since the estimation of individual internode length is accurate enough, this is mainly caused by the error existing in the number estimation of tertiary internodes and pedicels (Section Element quantity), which provides a feasible direction for the further improvement.

Reconstructed berry diameter indicated an error of 0.8 and 0.7 mm for Merlot bunches and Pinot Noir bunches, respectively, which remains acceptable. The berry volume is then available by using determined berry diameter, which facilitates relevant studies on the influence of berry size on viticultural productive index (bunch compactness, annual yield and wine flavour) comparing with the labour insensitive manual measurement of berry diameter.

Influence of different image capture orientations

In this subsection, left-view images of Merlot bunches were used to test the influence of the image capture orientation on the final reconstruction performance. Reconstruction results are shown in Figure 11 against results using front-view images. The performance of bunch element estimation, bunch topological architecture estimation and element property estimation is summarised in Table 9. For simplicity, corresponding reconstruction performance of same target bunches using front-view images as inputs was extracted and summarised in Table 10.

From the reconstruction results revealed in Figure 11, it is obvious that reconstructed models coming from left-view images are less similar to the real bunch when comparing with those coming from front-view images. Comparing with the results in Tables 9 and 10, there is no obvious change in the performance of internode length estimation, but a significant decrease has been found in the performance of pedicel number estimation by using left-view images as inputs. Since the number of pedicels (equal to the number of berries) is considered as an important trait of a bunch, a brief interpretation of the reason giving rise to this poor performance is as follows.

Table 9. Summary of the overall reconstruction performance using left-view images with respect to internode types of Merlot grapevine bunches

Evaluation metrics	**Rachis**	**Secondary**	**Tertiary**	**Pedicel**
Percentage error of internode number per bunch (%)	16.5	11.4	41.4	56.7
$F1$ Score	0.89	0.75	0.58	0.38
Percentage error of overall internode length (%)	11.1	13.1	4.3	0.2
Percentage error of individual internode length (%)	8.0	4.0	-7.5	0.4

Table 10. Summary of the overall reconstruction performance using front-view images with respect to internode types of Merlot grapevine bunches

Evaluation metrics	Rachis	Secondary	Tertiary	Pedicel
Percentage error of internode number per bunch (%)	28.3	13.3	35.7	26.4
$F1$ Score	0.87	0.82	0.64	0.48
Percentage error of overall internode length (%)	-1.3	23.4	-5.7	-2.9
Percentage error of individual internode length (%)	-2.8	2.4	-24.3	-3.8

Considering the branching system within the internode framework of a bunch, the order of importance for respective internode types is defined based on their parental relations (Section Topological reconstruction), where rachis internodes have a higher level than secondary internodes followed by tertiary internodes and pedicels. A higher position in the order of importance refers to containing more child internodes and thus a larger influence on the overall bunch architecture. As mentioned in Section Grapevine bunch measurements, images from different views lead to different bunch outlines, and therefore result in different outline hulls. Since the outline hull exerts constraints of overall shape and volume on the reconstructed model, changes in outline hull will undoubtedly influence the final result. Notice that the most significant difference between the front-view image and the left-view image of a bunch is the width of the shoulder (Figures 4, 11), a shorter width of shoulder will result in a lower number of reconstructed internodes on the first several secondary branches. Knowing that secondary internodes are at the second place in the order of importance, a slight change in the number of secondary internodes will exert a large influence on the prediction of corresponding child internodes, i.e. tertiary internodes and pedicels. Combining with the discovery in Pisciotta et al. (2013) that branches of the apical third of the rachis hold most berries of a bunch (43% of berries of a bunch), the reason for the poor reconstruction result by using left-view images can then be understood.

Whereas the proposed reconstruction method relies on 2D images and hence is dependent on image capture orientation, the input image has to be stipulated as the front-view image of the target, which lays a foundation for further improvement. An analysis of the image will be added to determine the image capture orientation and an improved reconstruction grammar will be employed in order to make our method suitable for input images other than the front view as well.

Conclusions

In this paper, we present a combination of grammar-based reconstruction and vision-based reconstruction, and proposed a new method for grapevine bunch reconstruction based on a well-established reconstruction grammar which is restricted by the outline hull formed from the boundary of a reference image. The proposed reconstruction grammar considered bunch architecture in two ways: topological reconstruction which focused on the connection relationships between elements, and geometrical reconstruction which stipulated exact properties for each element. The outline hull provides a terminal condition for the reconstruction grammar to stipulate the shape and volume of

the reconstructed model. The overall method was tested on 24 bunches including 20 bunches of Pinot Noir and four bunches of Merlot, and the result indicated that the proposed reconstruction method achieved a considerable improvement in aspects of candidate number estimation, candidate topology estimation and candidate property estimation, which can facilitate improvement to breeding programs and vineyard management. In particular, compared with existing works relying on 3D scanning, the proposed reconstruction method achieved a good accuracy by using only 2D information from the target bunch combined with an empirical model, which made it more convenient to be applied under field conditions.

Further improvements will be possible through the following: enlarging the dataset by including more bunch samples from different cultivars with full measurements; integrating reconstruction rudiments for different shapes of bunches into the reconstruction grammar in order to extend the transferability of the proposed work. Furthermore, since measurement of bunches is unavoidable, future work is needed to automate the measurement of internode framework in a reliable way as it is exceptionally tedious. Some other improvements will be conducted as well to make the method less sensitive to the image capture orientation.

References

Barbetti, M. J. (1980) Reductions in bunch rot in Rhine Riesling grapes from bunch thinning. Australasian Plant Pathology **9(2)**, 8–10.

Clingeleffer, P., Dunn, G., Krstic, M. and Marin S. (2001) Crop development, crop estimation and crop control to secure quality and production of major wine grape varieties: a national approach. Technical report, (Grape and Wine Research and Development Corporation: Adelaide, SA, Australia).

Doligez, A., Bququet, A., Danglot, Y., Lahogue, F., Riaz, S., Meredith, C. P., Edwards, K. J. and This, P. (2002) Genetic mapping of grapevine (*Vitis vinifera* L.) applied to the detection of QTLs for seedlessness and berry weight. Theoretical and Applied Genetics 105, 780–795.

Fanizza, G., Lamaj, F., Costantini, L., Chaabane, R. and Grando, M. S. (2005) QTL analysis for fruit yield components in table grapes (*Vitis vinifera*). Theoretical and Applied Genetics. **111,** 658–664.

Fermaud, M. (1998) Cultivar susceptibility of grape berry clusters to larvae of lobesia botrana (Lepidoptera: Tortricidae). Journal of Economic Entomology **91**, 974–980.

Font, D., Tresanchez, M., Martínez, D., Moreno, J., Clotet, E. and Palacín, J. (2015) Vineyard yield estimation based on the analysis of high resolution images obtained with artificial illumination at night. Sensors **15**, 8284–8301.

Godin, C. (2000). Representing and encoding plant architecture: a review. Annals of Forest Science **57**, 413–438.

Furbank, R. T., Tester, M., (2011) Phenomics – technologies to relieve the phenotyping bottleneck. Trends Plant Science **16**, 635–644.

612 Hed, B., Ngugi, H. K. and Travis, J. W. (2011) Use of gibberellic acid for management of bunch rot on
613 chardonnay and vignoles grape. Plant disease **95**, 269–278.

614 Herrero-Huerta, M., González-Aguilera, D., Rodriguez-Gonzalvez, P. and Hernández-López, D. (2015)
615 Vineyard yield estimation by automatic 3d bunch modelling in field conditions. Computers and
616 Electronics in Agriculture **110,** 17–26.

617 Herzog, K. (2014) Initial steps for high-throughput phenotyping in vineyards. Australian & New Zealand
618 Grapegrower & Winemaker (**603)**, 54.

619 Herzog, K., Wind, R. and Töpfer, R. (2015) Impedance of the grape berry cuticle as a novel phenotypic
620 trait to estimate resistance to Botrytis cinerea. Sensors **15**, 12498-12512.

621 Huang, C. Y., Jheng, W. T., Tai, W. K., Chang, C. C. and Way, D. L. (2013) Procedural grape bunch
622 modeling.Computers & Graphics **37** , 225–237.

623 Kicherer, A., Roscher, R., Herzog K., Šimon, S., Fröstner, W. and Töpfer, R. (2013) BAR (Berry Analysis
624 Tool): a high-throughput image interpretation tool to acquire the number, diameter, and volume of
625 grapevine berries, Vitis **52**, 129–135.

626 Liu, S., Whitty, M. and Cossell, S. (2015) A lightweight method for grape berry counting based on auto-
627 mated 3D bunch reconstruction from a single image Workshop on robotics in agriculture; 30 May 2015;
628 Seattle, USA.

629 Mack, J., Lenz, C., Teutrine, J. and Steinhage, B. (2017) High-precision 3D detection and reconstruction
630 of grapes from laser range data for efficient phenotyping based on supervised learning. Computers
631 and Electronics in Agriculture **135,** 300–311.

632 May, P. (2005) Flowering and fruitset in grapevines. Phylloxera and Grape Industry Board of South
633 Australia in association with Lythrum Press: Adelaide, SA, Australia.

634 Měch, R. and Prusinkiewicz, P. (1996) Visual models of plants interacting with their environment.
635 Proceedings of the 23rd annual conference on computer graphics and interactive techniques;
636 Publisher: Association for computing machinery; August 1996; New York, USA; pp. 397–410.

637 Nuske, S., Achar, S., Bates, T., Narasimhan, S. and Singh, S. (2011) Yield estimation in vineyards by
638 visual grape detection; Proceedings of 2011 IEEE/RSJ International Conference on Intelligent Robots
639 and Systems (IROS); IEEE; 9-13 May 2011; Shanghai, China; pp. 2352–2358.

640 Nuske, S., Gupta, K., Narasimhan, S. and Singh, S. (2014) Modeling and calibrating visual yield
641 estimates in vineyards; Field and Service Robotics. pp. 343–356.

642 Organisation Internationale de la Vigne et du Vin (2009) Descriptor list for grape varieties and Vitis
643 species. Organisation Internationale de la Vigne et du Vin (OIV),
644 http://www.oiv.int/public/medias/2274/code-2e-edition-finale.pdf

645 Pisciotta, A., Di Lorenzo, R., Barbagallo, M. G. and Hunter, J. J. (2013) Berry characterisation of cv Shiraz
646 according to position on the rachis. South African Journal of Enology and Viticulture **34(1)**, 100-107.

Pratt, C. (1971) Reproductive anatomy in cultivated grapes - a review. American journal of enology and viticulture **22,** 92–109.

Prusinkiewicz, P., James, M. and Měch, R. (1994) Synthetic topiary. Proceedings of the 21st annual conference on computer graphics and interactive techniques; Association for computing machinery; New York, USA; pp. 351–358.

Prusinkiewicz, P., Műndermann, L., Karwowski, R. and Lane, B. (2001) The use of positional information in the modeling of plants. Proceedings of the 28th annual conference on computer graphics and interactive techniques; Association for computing machinery; May 2001; New York, USA; pp. 289–300.

Rist, F., Herzog, K., Mack, J., Richter, R., Steinhage V. and Töpfer R. (2018) High-precision phenotyping of grape bunch architecture using fast 3D sensor and automation. Sensors **18**, 763.

Rose, J. C., Kicherer, A., Wieland, M., Klingbeil, L., T¨opfer, R. and Kuhlmann, H. (2016) Towards automated large-scale 3D phenotyping of vineyards under field conditions. Sensors **16**, 2136–2160.

Schnabel, R., Wahl, R. and Klein, R. (2007) Efficient RANSAC for point-cloud shape detection. Computer Graphics Forum **26**, 214–226.

Schöler, F. and Steinhage, V. (2015). Automated 3d reconstruction of grape cluster architecture from sensor data for efficient phenotyping. Computers and Electronics in Agriculture **114,** 163–177.

Shavrukov, Y., Dry, I. B. and Thomas, M. R. (2004) Inflorescence and bunch architecture development in vitis vinifera l. Australian Journal of Grape and Wine Research **10**, 116–124.

Tello, J., Cubero, S., Blasco, J., Tardauila, J., Aleixos, N. and Ibáñez, J. (2015) Application of 2D and 3D image technologies to characterise morphological attributes of grapevine clusters. Journal of the Science of Food and Agriculture **96**, 4575-4583.

Troll, W., (1952) Die Infloreszenzen. Typologie und Stellung im Aufbau des Vegetationskorpers. G. Fischer, Stuttgart.

Vail, M. E., Wolpert, J. A., Gubler, W. D. and Rademacher, M. R. (1998) Effect of cluster tightness on botrytis bunch rot in six Chardonnay clones. Plant Disease **82**, 107–109.

Weaver, R. J., Kasimatis, A. N. and Mccune, S. B. (1962) Studies with gibberellin on wine grapes to decrease bunch rot. American Journal of Enology and Viticulture **13** , 78–82.